12A.5

RAINBANDS AND SECONDARY EYE WALL FORMATION AS OBSERVED IN RAINEX

Derek Ortt* and Shuyi S. Chen
RSMAS, University of Miami, Miami FL

1. INTRODUCTION

The formation of secondary eye walls in tropical cyclones (TC) and a subsequent contraction of the secondary eye wall as the primary eye wall weakens is known as an eye wall replacement cycle (EWRC) (Willoughby et al. 1982). The first recorded case of a EWRC was in Typhoon Sarah (Fortner, 1958). Later studies documented that this process was associated with significant intensity changes in TCs. However, despite a number of studies on this topic, the causes of a EWRC remains an unanswered question. Previous studies have examined either the inner-core, or outer rainband region (e.g. Samsury and Zisper, 1995), but not the interactions of the core with the rainbands, which may be key to understanding EWRCs. This shortcoming was addressed by the Hurricane Rainband and Intensity Experiment (RAINEX).

RAINEX conducted the first simultaneous sampling of the outer rainband region and the inner-core of a TC, using three P3 aircraft with Doppler radar and dropsonde capabilities, including a Navy P3 aircraft and two National Oceanic and Atmospheric Administration (NOAA) aircraft. The three aircraft were able to collect valuable dropsonde data in Hurricanes Katrina and Rita (2005). In addition, RAINEX conducted real-time high resolution model forecasts for both mission planning and post-mission analysis.

The objective of this study is to examine characteristics of the rainband and its environmental conditions in the two hurricanes. Rita underwent a EWRC in the Gulf of Mexico while under observation by RAINEX, whereas Katrina did not. The vertical profiles of moisture, temperature, and winds from both the aircraft dropsondes and the model simulations will be used to determine the key features of the rainbands in the hurricanes. The goal is to determine what role, if any, the low-level moisture near the outer rainbands plays in the generation of a EWRC.

* Corresponding author address: 4600 Rickenbacker Causeway. Miami, FL 33143. E-mail: dortt@rsmas.miami.edu.

2. DATA AND METHOD

The data used in this study are the GPS dropsonde data from the three P3 aircraft. The dropsonde data has a .5 second resolution (Franklin et al., 2003). For this study, the data was interpolated onto a 25m resolution from the surface to 2.5km. Only dropsondes from the outer rainband region are included. NOAA and Navy aircraft flew inside and outside of the principle rainband, in a pattern to that shown in figure 1. Dropsondes were deployed along the flight track.

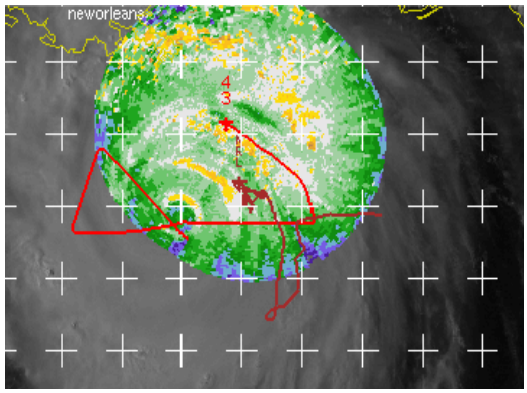

Figure 1: Flight track of NOAA-43 and the NRL P-3 in Hurricane Katrina during the afternoon of August 28, 2005.

The corresponding vertical profiles from the model forecasts are used to compare with the dropsonde data. The model data used for the real-time forecasts is the 5th generation PSU-NCAR non-hydrostatic mesoscale model (MM5) with a vortex following nested grid developed by Chen and Tenerelli (2006). The Katrina simulation used GFDL initial and boundary conditions and began at 0000 UTC, August 27, 2005, while the Rita simulation used NOGAPS initial and boundary conditions and began at 0000 UTC, September 20, 2005. The rainband

region in both simulations had a horizontal resolution of 5km and a 28 sigma level vertical resolution. Both simulations required the extraction of a vortex of the appropriate initial intensity from a previous simulation, and inserting this vortex into our simulations at the initial time.

The dropsonde data analysis included the compositing of all of the temperature, mixing ratio, and relative humidity (RH) data for Hurricanes Katrina and Rita, and comparing the composite results for each storm. The same method was used for analyzing the data from the simulations. Exact storm relative locations in the simulations could not be used because the simulations did not reproduce the observed vortex size and rainband locations with 100 percent accuracy. Therefore, the model was sampled between the rainbands similar as to how the aircraft sampled the observed hurricanes. The locations of the simulation profiles are near aircraft dropsonde locations, though additional simulation locations were sampled to provide more complete coverage of the entire storm. Figure 2 shows an example of where the model profiles were taken.

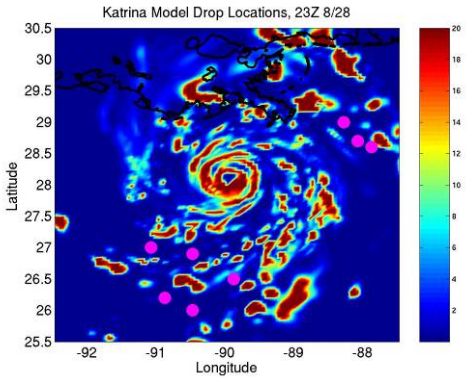

Figure 2: Example of model vertical profile locations. The magenta dots represent the locations where the simulated drops were taken.

3. RESULTS

GPS dropsonde data shows Hurricane Rita having an environment closer to saturation than Hurricane Katrina. The RH difference was greatest near the top of the boundary layer, where the composite RH for Hurricane Rita was nearly 10% higher than Hurricane Katrina. This signal persists to about 2km, where the RH differences decrease to less than 5 percent.

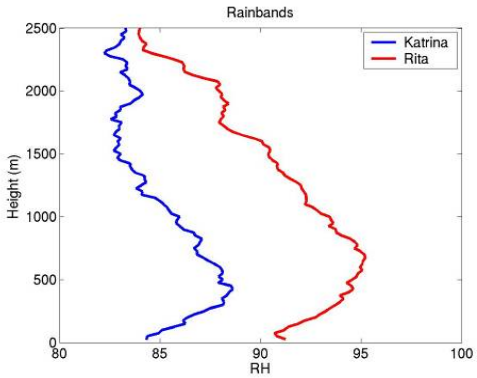

Figure 3: Composite vertical RH profiles for Hurricanes Katrina and Rita from GPS dropsondes. Katrina is in blue, Rita is in red.

The RH differences shown above are at least partially attributable to there being more total liquid water for Hurricane Rita than Katrina. The composite mixing ratio for Hurricane Rita was .5 to 1 g/kg above that of Katrina in much of the lower troposphere.

Preliminary simulation results show that the simulated Katrina and Rita were similar to the observed hurricanes. Similar to the dropsonde observations, the simulation of Hurricane Rita had a rainband region closer to saturation than did Hurricane Katrina. As was the case for the dropsondes, the model composite mixing ratio was higher for Rita above the boundary layer.

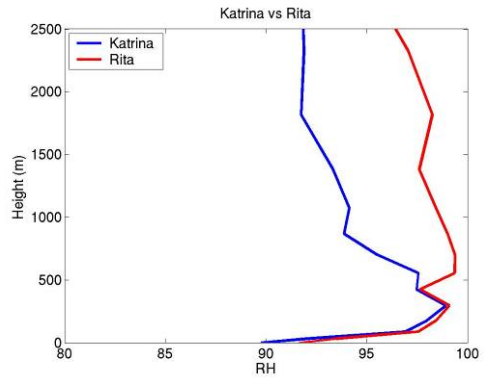

Figure 4: Composite model RH profiles.

These results indicate that an atmosphere closer to saturation is more favorable for a EWRC. This idea was introduced by Nong and Emanuel (2003) via numerical modeling studies. A possible physical reason for this is an environment closer to saturation allows for more latent heat release, which allows increased vertical velocity as the air is more buoyant. Since du/dx+dv/dy=-dw/dz, the increased vertical

motion results in greater low-level convergence, resulting in enhanced vorticity outside of the primary eye wall. Kossin et al. (2000) suggested that a secondary ring of enhanced vorticity can lead to the formation of a secondary eye wall.

4. CONCLUSION

Based upon the dropsonde and model data, it appears as if an environment that is near or at saturation and is relatively stable favors the formation of a concentric eye wall. Future research will examine other storms to determine if this signal is a coincidence between these two storms, or a robust signal that applies to all TCs.

Acknowledgements: We would like to thank NOAA-HRD for providing the NOAA P-3 data and NCAR for the Navy P-3 data. The research is supported by a NSF grant ATM-0432717. The first author is supported by an American Meteorological Society Fellowship and a University of Miami fellowship.

References:

Chen, S. S., and J. E. Tenerelli, 2006: Simulation of hurricane lifecycle and inner-core structure using a vortex following mesh refinement: Sensitivity to model grid resolution. *Mon. Wea. Rev.*, in revision.

Fortner, L.E., 1958: Typhoon Sarah, 1956. *Bull. Amer. Meteor. Soc.,* **39,** 633-639.

Franklin, J. L., M. L. Black, K. Valde, 2003: GPS dropwindsone profiles in hurricanes and their operational implications. *Weather and Forecasting* **18,** 32-44

Kossin, J.P., W. H. Schubert, and M.T. Montgomery, 2000: Unstable interactions between a hurricane's primary eyewall and a secondary ring of enhanced vorticity. *J. Atmos. Sci.,* **57,** 3893-3917.

Nong, S. and K. Emanuel, 2003: A numerical study of the genesis of concentric eyewalls in hurricanes. *Q. J. R. Met. Soc.,* **129,** 3323-3338.

Samsury, C. E. and E. J. Zipser, 1995: Secondary wind maxima in hurricanes: Airflow and relationship to rainbands. *Mon. Wea. Rev.*, **123**, 3502-3517.

Willoughby, H. E., J. A. Clos, and M. G. Shoreibah, 1982: Concentric eyewalls, secondary wind maxima, and the evolution of the hurricane vortex. *J. Atmos. Sci.*, **39**, 395-411